

In the iron(III) case the mechanistic change is most pronounced: from  $I_a$  for  $\text{Fe}(\text{H}_2\text{O})_6^{3+}$  to  $I_d$  for  $\text{Fe}(\text{H}_2\text{O})_5(\text{OH})^{2+}$ . In  $\text{Ru}(\text{H}_2\text{O})_6^{3+}$  the associative character is stronger; therefore, the mechanistic change toward dissociation is less pronounced in  $\text{Ru}(\text{H}_2\text{O})_5(\text{OH})^{2+}$ . At the transition state both bond making and bond-breaking (I mechanism) contribute equally to the activation volume.

**Acknowledgment.** We thank the Swiss National Science Foundation for financial support (Grants 2.854-0.85 and 2.209-0.81) and CIBA-GEIGY AG for elemental analyses.

**Registry No.**  $\text{Ru}(\text{H}_2\text{O})_6^{2+}$ , 30251-71-9;  $\text{Ru}(\text{H}_2\text{O})_6^{3+}$ , 30251-72-0;  $\text{Ru}(\text{H}_2\text{O})_5\text{OH}^{2+}$ , 73663-64-6;  $\text{Ru}(\text{CH}_3\text{CN})_6^{2+}$ , 53139-84-7;  $\text{H}_2\text{O}$ , 7732-18-5;  $\text{CH}_3\text{CN}$ , 75-05-8.

**Supplementary Material Available:** Water exchange rate constants and oxygen-17 quadrupolar relaxation rates of  $\text{Ru}(\text{H}_2\text{O})_6^{2+}$  as a function of temperature (Table SI) and pressure (Table SII), acetonitrile exchange rate constants of  $\text{Ru}(\text{CH}_3\text{CN})_6^{2+}$  as a function of temperature and pressure (Table SIII), oxygen-17 transverse relaxation rates of  $\text{Ru}(\text{H}_2\text{O})_6^{3+}$  as a function of temperature and acidity (Table SIV), and pH dependence of the absorbance of a  $\text{Ru}(\text{H}_2\text{O})_6^{3+}$  solution (Table SV) (4 pages). Ordering information is given on any current masthead page.

Contribution from the Institute of Inorganic Chemistry, Technical University of Aachen, D-5100 Aachen, FRG, and Institute of Physical Chemistry II, Ecole Polytechnique Fédérale de Lausanne, CH-1015 Lausanne, Switzerland

## Kinetics and Mechanism of the Reduction of Protons to Hydrogen by Cobaltocene

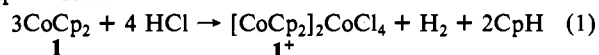
U. Koelle,\*† P. P. Infelta,‡ and M. Grätzel†

Received February 2, 1987

The rate constant  $k_{\text{obsd}}$  for the overall reaction  $2\text{CoCp}_2 + 2\text{H}^+ \rightarrow 2\text{CoCp}_2^+ + \text{H}_2$  (eq i) was determined by pulse radiolysis in an aqueous sulfuric acid medium for cobaltocene (**1**), 1,2,3,4,5-pentamethylcobaltocene (**2**), and decamethylcobaltocene (**3**). The reaction is first order in **1** and in protons with  $k_{2,\text{obsd}} = 42 \pm 1.5 \text{ s}^{-1} \text{ M}^{-1}$  at  $c_{\text{H}^+} = 8 \times 10^{-3}$ – $4.7 \times 10^{-1} \text{ M}$ . Possible mechanistic pathways for eq i are discussed, and a second-order disproportionation of protonated **1** or a mechanism that involves reduction of protonated **1** by unprotonated **1** is best compatible both with the observed kinetics and with chemical evidence. Deuteration experiments show protonation to occur exclusively at the metal.

### Introduction

From the beginning of cobaltocene chemistry one of the most intriguing reactions of this electron-rich sandwich complex has been the one with acids.<sup>1,2</sup> Reports from different laboratories noted a somewhat different course of the reaction depending on the acid employed. Thus, whereas aqueous HCl led to the formation of a tetrachlorocobaltate with partial decomplexation of Co (eq 1),<sup>3</sup> a clean oxidation of **1** to  $\text{1}^+$  with acids having a noncoordinating anion such as  $\text{HBF}_4$  and  $\text{HPF}_6$  was found.<sup>4</sup> We observed that also acids like  $\text{H}_2\text{SO}_4$ ,  $\text{CH}_3\text{COOH}$ , and  $\text{CF}_3\text{COOH}$  in water and polar organic solvents exclusively reacted according to eq 2. Reaction 2 is of interest as a model reaction for the



reduction of protons by a transition-metal complex. Since it is a noncomplementary electron-transfer reaction, its mechanism must be complex. Visually the reaction of **1** with 0.1 M  $\text{HBF}_4$ ,  $\text{H}_2\text{SO}_4$ , or  $\text{CF}_3\text{COOH}$  in THF/water is complete in the time of mixing at ambient temperature without noticeable formation of intermediates.

Evaluation of the kinetics of reaction 2 faces two major problems. Since the kinetics are too fast to be followed by conventional spectrophotometry, the air sensitivity of cobaltocene at the low concentrations available in water (estimated  $10^{-5} \text{ M}$ ) precludes its handling in all but rigorously closed systems. Since oxidations by protons or oxygen are spectrophotometrically indistinguishable, minor traces of oxygen would interfere with the kinetics. These difficulties are overcome by reducing the cobaltocenium cation  $\text{1}^+$  with electrons or reducing radicals, generated in an electron pulse, in acidic aqueous solution to neutral cobaltocene and monitoring the absorption decay of the latter when reaction 2 proceeds.

In addition to the pulse radiolysis experiments performed along these lines, results of the oxidation of **1** and its 1,2,3,4,5-penta-

methyl derivative, **2**, by  $\text{CH}_3\text{COOH}$  in ethanol, monitored by using conventional spectrophotometry, are presented. The reaction of **1** with  $\text{CF}_3\text{COOH}$  in  $\text{CH}_3\text{OD}$  was studied to probe the site of protonation.

### Experimental Section

For electrochemical measurements EG&G/PAR equipment (Model 173 potentiostat/galvanostat and Model 174A polarographic analyzer) was used. Cyclic voltammograms in ethanol/ $\text{H}_2\text{SO}_4$ / $\text{Na}_2\text{SO}_4$  were recorded on a hanging-mercury-drop electrode (EG&G/PAR SMDE 303). Bulk electrolysis of  $\text{1}^+$  was performed in a divided cell at a mercury-pool cathode. The electrolyte consisted of an aqueous surfactant solution ( $4 \times 10^{-3} \text{ M C}_n\text{F}_{2n+1}\text{SO}_3\text{H}^+$ ) and 0.1 M  $\text{LiClO}_4$  as the supporting electrolyte.

Samples for pulse radiolysis were prepared by Ar-degassing ( $1$ – $5 \times 10^{-3} \text{ M}$ ) aqueous solutions of [**1**–**3**]Cl in  $1 \times 1 \text{ cm}$  quartz cells fitted with gastight rubber septums and containing varying concentrations of sulfuric acid and 10% v/v of 2-propanol.<sup>6</sup> The cells were placed in the beam of the 3-MeV Van de Graaff (horizontal) accelerator of the EPFL. The pulse length was 500 ns. A 450-W high-pressure Xe arc lamp and a 320-nm cutoff filter were employed for illumination, and the monochromated light was detected with a Hamamatsu photomultiplier (PM) operated at 700–800 V. By means of a shutter system the sample was exposed to the arc light only a few seconds before and after the pulse to avoid heating and photolysis. Provision was made for magnetic stirring in cases where the decay of neutral **1** was slow in order to establish homogeneous conditions in the sample prior to each pulse. The output from the PM was sampled by a Tektronix digital storage oscilloscope and transferred to an HP 85 calculator to perform automatic first- and second-order analysis of the trace. The upper limit for the time scale of the experiment, determined by lamp instabilities and diffusive broadening of the beam volume, is on the order of 1 s, which confines the observation

(1) See: Kemmit, W. R.; Russell, D. R. In *Comprehensive Organometallic Chemistry*; Stone, F. G. A., Abel, W. E., Eds.; Academic: Oxford, England, 1982; Vol. 5, p 246 ff.

(2) See: Sheets, J. E. *J. Organomet. Chem.* 1979, 64.

(3) (a) Miyake, A.; Kondo, H.; Aoyama, M. *Angew. Chem., Int. Ed. Engl.* 1969, 8, 520. (b) van Akker, M.; Jellinek, F. *Recl. Trav. Chim. Pays-Bas* 1971, 90, 1101.

(4) Salzer, A., University of Zürich, private communication.

(5) A mixture of fluorinated sulfonic acids,  $\text{C}_n\text{F}_{2n+1}\text{SO}_3\text{H}$ , with  $n$  ranging from 4 to 8 was kindly supplied by Hoechst AG, Frankfurt/Main, FRG.

(6) 2-Propanol was found superior to formic acid or  $\text{Zn}^{2+}$  as a quencher of  $\text{OH}^\cdot$  in the acidic medium.

\* Technical University of Aachen.

† Ecole Polytechnique Fédérale de Lausanne.

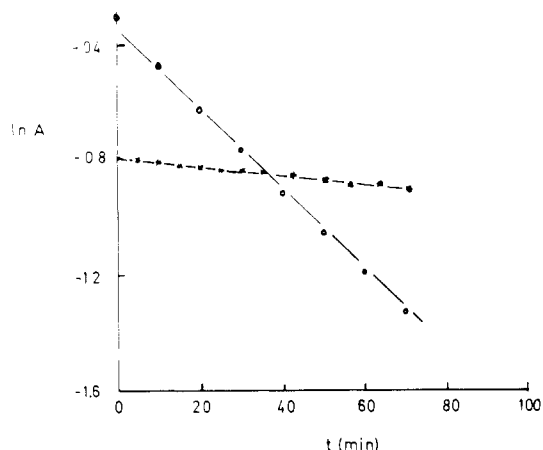


**Figure 1.**  $\log A$  vs  $t$  for reaction 2 of cobaltocenes **1** (---\*) and **2** (—○) in EtOH/CH<sub>3</sub>COOH. For experimental conditions, see text.

of reaction 2 to proton concentrations in excess of  $10^{-2}$  M.

A comparison of the rates of reaction 2 for **1** and **2** was achieved by following the absorption change on a Cary 219 spectrophotometer of **1** ( $9 \times 10^{-3}$  M) and **2** ( $6.4 \times 10^{-3}$  M), respectively, in ethanol containing 0.44 M CH<sub>3</sub>COOH and 0.1 M CH<sub>3</sub>COONa (a buffer composition that would give pH 4 in water) at 370 nm in a 0.1-cm Schlenk-fitted optical cell. From the straight-line  $\log A$  vs  $t$  plot shown in Figure 1 pseudo-first-order rate constants  $k_1' = 9 \times 10^{-6}$  s<sup>-1</sup> for **1** and  $2.8 \times 10^{-4}$  s<sup>-1</sup> for **2**, respectively, were obtained. In an analogous experiment the complex CoCp(C<sub>5</sub>H<sub>6</sub>) was treated with CH<sub>3</sub>COOH and found not to react with acid under these conditions. Reaction of **1** with CF<sub>3</sub>COOD was conducted in a 100-mL Schlenk flask fitted with a gastight rubber septum. The flask was charged with 1.09 g (5.76 mmol) of **1** and 10 mL of CH<sub>3</sub>OD with a nominal deuteration degree of 99%. The mixture was cooled to 100 K and evaporated to  $10^{-3}$  Torr. After this sample was warmed to 250 K, 1.6 mL (21.5 mmol) CF<sub>3</sub>COOD was added by syringe and the mixture stirred for 1/2 h at ambient temperature until the solution was homogeneous and of light brown color. The gas volume was analyzed for H<sub>2</sub>/HD/D<sub>2</sub> by mass spectrometry, and the ratio of isotopic composition found was (in this order) 1:2.85:10.45. The solvent was then condensed into a separate flask, the residue dissolved in water and filtered, and the cobaltocenium cation precipitated as the hexafluorophosphate. After it was dried, 250 mg (0.75 mmol) of the salt was reduced to neutral **1** by stirring it with 170 mg (0.65 mmol) of pentamethylcobaltocene (**2**) in 10 mL of THF.<sup>7</sup> After evaporation of the solvent **1** was sublimed from the residual cobaltocenium salt and subjected to mass spectrometric investigation. The ratio of peaks with  $m/e$  189 and 190 was found to be 100:14 as required by <sup>13</sup>C isotopic composition alone and was identical with the M:(M + 1) ratio of an undeuterated sample. Likewise, the IR spectrum of the isolated cobaltocenium salt was identical with that of an undeuterated sample and was devoid of any additional absorptions due to C-D stretching modes in the 1900–1600-cm<sup>-1</sup> region.

## Results

**Electrochemical Measurements.** At acid concentrations that allow the reduction of **1**<sup>+</sup> in ethanolic sulfuric acid to be observed separated from direct proton reduction ( $< 2 \times 10^{-2}$  M) at a hanging-Hg-drop electrode, anodic/cathodic peak-current ratios of the cyclic voltammogram are only slightly below unity, allowing but an upper value for a first-order follow-up rate constant to be estimated as  $k_f < 6 \times 10^{-2}$  s<sup>-1</sup> at  $c_{H^+} = 10^{-2}$  M. In line with this rather slow rate the polarographic curve for the reduction of **1**<sup>+</sup> in an acidified solution did not show the characteristics of a catalytic wave. Electrochemically reaction 2 is best demonstrated by the sustained electrolysis of **1**<sup>+</sup> in acidic aqueous micellar<sup>5</sup> solution at a Hg-pool cathode, where hydrogen can be produced continuously at a potential 200 mV positive of the onset of direct

(7) Reduction of **1**<sup>+</sup> in this experiment must be effected with a neat electron-transfer reductant slightly negative of the **1**<sup>+/0</sup> redox potential as supplied by the pentamethyl derivative **2**. Na/Hg for example would be unsuited since the cobaltocenate anion, which is easily produced by this reductant, protonates to CoCp(C<sub>5</sub>H<sub>6</sub>) (**4**), which has the same molecular weight as the anticipated CoCpC<sub>5</sub>H<sub>6</sub>D and would thus interfere with the diagnostic M:(M + 1) ratio in the mass spectrum.

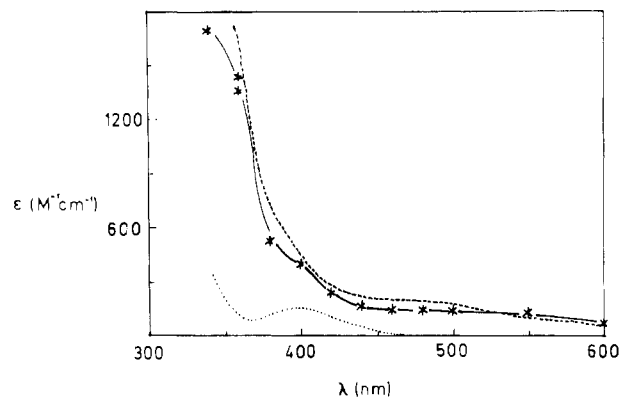
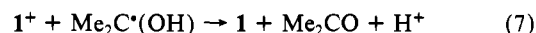
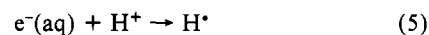
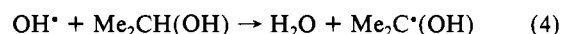
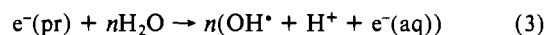


**Figure 2.** Absorption spectra of **1** (---) and **1**<sup>+</sup> (···) in EtOH and of the species generated from **1**<sup>+</sup> by the electron pulse (—\*—).

proton reduction. When **1**<sup>+</sup> is electrolyzed at neutral pH, a brown, air-sensitive micellar solution of neutral **1** results, which is stable under nitrogen and does not react with water.

**Pulse Radiolysis. (a) Cobaltocene.** As outlined above, pulse radiolytic reduction of **1**<sup>+</sup> in a closed optical cell was chosen as a method to follow the oxidation of **1** by protons without interference of oxygen. An absorption spectrum of the species generated within <5 ms after the pulse is shown in Figure 2 and is identified as **1** by comparison with the spectrum of an authentic sample taken in ethanol. Included in Figure 2 is the spectrum of **1**<sup>+</sup> to illustrate the absorption difference between the neutral and the oxidized form in the wavelength range 340–400 nm, which allows for a convenient spectrophotometric determination of the former in the presence of a large excess of the latter. From the known absorption coefficient of **1** ( $1750$  cm<sup>-1</sup> M<sup>-1</sup> at 360 nm<sup>8</sup>) and the diameter of the electron beam (1 cm) the initial concentration of **1**,  $c_0$ , generated by a 500-ns pulse at 3 MeV, corresponding to a total charge of  $4 \times 10^{-8}$  C, is calculated as  $8 \times 10^{-6}$  M. It linearly follows the beam intensity from  $4 \times 10^{-8}$  to  $4 \times 10^{-7}$  C. In this concentration range ( $8 \times 10^{-6}$ – $8 \times 10^{-5}$  M)  $k_{\text{obsd}}$  at constant  $c_{H^+}$  is independent of  $c_0$ , indicating a first-order reaction in cobaltocene.

Generation of **1** is thought to proceed by reactions 3–7 with Me<sub>2</sub>C\*(OH) as the reducing species. If, at higher pH, reaction



5 was incomplete, **1**<sup>+</sup> could be reduced by e<sup>-</sup>(aq) directly. Because of similar  $G$  values ( $G_e^- = 2.6$ ,  $G_{H^+} = 2.9$ ) for the generation of e<sup>-</sup>(aq) and H<sup>+</sup> in (3) the concentration of H<sup>+</sup> produced by the pulse never exceeds the cobaltocene concentration, which is  $\approx 10^{-5}$  M, and thus does not make any noticeable contribution to the acidity of the medium within the beam volume.

Whereas at pH > 2.5 the absorption due to **1**, as generated by the pulse, is rather persistent, at pH < 2 the cobaltocene signal, monitored at 340 nm, decays progressively faster with increasing proton concentration, following first-order kinetics for more than 3 half-lives. Figure 3 reproduces an experimental decay curve and its log plot. Note that the absorption decay is to the initial value, indicating quantitative reversion to the starting product. Thus, traces of oxygen, initially present in the sample, are consumed after a few electron pulses and the decay of **1** attains a constant rate. Table I collects  $k_{\text{obsd}}$  at different proton concentrations. In Figure 4  $k_{\text{obsd}}$  is plotted vs the proton concentration, giving a straight line ( $r = 0.997$ ) with zero intercept and slope  $42.5 \pm 1.5$  s<sup>-1</sup> M<sup>-1</sup>.

(8) Koelle, U.; Infelta, P. P.; Grätzel, M., to be submitted for publication.

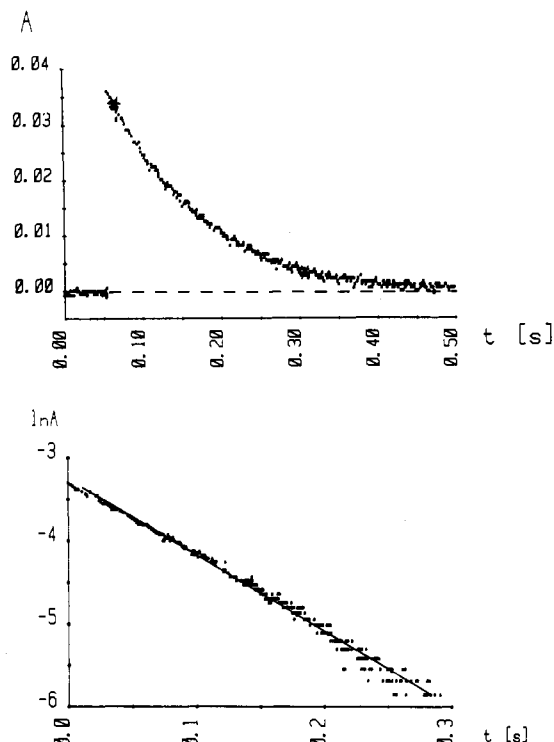


Figure 3. Generation and decay of **1** in pulse radiolysis.

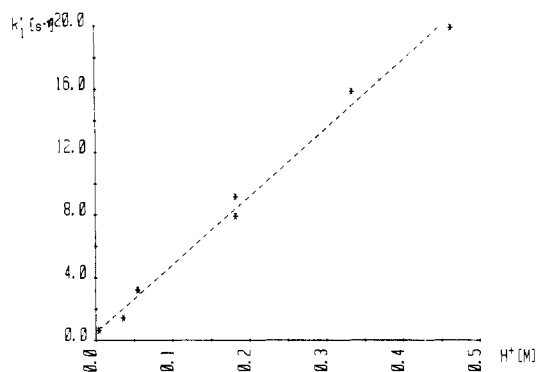


Figure 4.  $k_{\text{obsd}}$  ( $\text{s}^{-1}$ ) vs  $\text{H}^+$  for reaction 2 of **1**.

When beam intensities in excess of  $4 \times 10^{-7}$  C are used for pulsing, the kinetic pattern changes. The absorption decay is now biphasic with one rate comparable to the one at lower intensity, and a second one slower by 1 order of magnitude.

(b) **Pentamethyl- (2)<sup>9</sup> and Decamethylcobaltocene (3).**<sup>10</sup> Pulse radiolysis with aqueous solutions of **2<sup>+</sup>** and **3<sup>+</sup>** proved to be more complicated. Since the absorption of the cations **2<sup>+</sup>** and **3<sup>+</sup>** as compared to that of **1<sup>+</sup>** is much higher in the wavelength region 340–400 nm ( $\epsilon_{360} = 250 \text{ cm}^{-1} \text{ M}^{-1}$  for **2<sup>+</sup>** as compared to  $87 \text{ cm}^{-1} \text{ M}^{-1}$  for **1<sup>+</sup>**), the sensitivity (because of a lower light intensity  $I_0$ ) at 340–360 nm is lowered and the neutral sandwich complexes were monitored at wavelengths above 380 nm, where the absorption difference is smaller. Moreover, reduction of the methylated cobaltocenium cations with more negative redox potentials<sup>9,10</sup> proceeded with lower yields. Thus the initial concentration for e.g. **2** is estimated as  $4 \times 10^{-6} \text{ M}$ , which is about one-fifth of the initial concentration of **1** generated under the same conditions (Table I). As can be seen from Figure 5, the decay of the neutral complex is now at least biphasic. The rapid decay, which accounts for about half to one-third<sup>11</sup> of the total con-

Table I. Initial Cobaltocene Concentration  $c_0$ , Proton Concentration  $c_{\text{H}^+}$ , and Pseudo-First-Order Rate Constants  $k_{\text{obsd}}$  for Reaction 2 of Cobaltocenes 1–3

Complex 1		
$c_0(\mathbf{1})/10^{-5} \text{ M}$	$c_{\text{H}^+}/\text{M}$	$k_{\text{obsd}}/\text{s}^{-1}$
1.9	$8.1 \times 10^{-3}$	0.64
2.26	$3.2 \times 10^{-2}$	1.43
2.0	$5.8 \times 10^{-2}$	3.21
2.2	$1.9 \times 10^{-1}$	9.16
1.0	$1.9 \times 10^{-1}$	7.91
1.4	$3.4 \times 10^{-1}$	15.8
2.0	$4.7 \times 10^{-1}$	19.8
Complex 2 <sup>b</sup>		
$c_{\text{H}^+}/\text{M}$	$k_{\text{obsd}}/\text{s}^{-1}$	$k'_{\text{obsd}}/\text{s}^{-1 a}$
$3.2 \times 10^{-2}$	166	6.8
$5.8 \times 10^{-2}$	356	8.8
$5.8 \times 10^{-2}$	330	2.0
$3.4 \times 10^{-1}$	730	0.5
Complex 3 <sup>b</sup>		
$c_{\text{H}^+}/\text{M}$	$k_{\text{obsd}}/\text{s}^{-1}$	$k'_{\text{obsd}}/\text{s}^{-1 a}$
$8.1 \times 10^{-3}$	300	18
$3.2 \times 10^{-2}$	720	19

<sup>a</sup> Pseudo-first-order rate constant of the slow decay; see text. <sup>b</sup> Initial concentration difficult to estimate due to low signal intensity but estimated to be  $4 \times 10^{-6} \text{ M}$ .

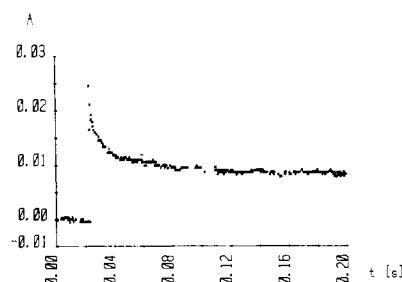


Figure 5. Generation and decay of **2** in pulse radiolysis.

centration change has rates that exceed the decay rate of **1** by a factor of 100 (Table I). This rapid decay qualitatively follows the proton concentration. The residual absorption decays much slower with rate constants  $0.5\text{--}5 \text{ s}^{-1}$ , which do not follow the proton concentration. The spectrum of the slowly decaying species, taken between 370 and 650 nm, shows an extension to longer wavelengths as compared to that of **1** or the methylated cobaltocenes and must be assigned to an intermediate.

#### Discussion

A discussion of possible mechanisms of reaction 2 has to start with the site of protonation, the metal or a Cp ring. Either reaction type can be found in the literature. Thus, ferrocene<sup>12</sup> is reported to protonate at the metal as appears generally to be the case with  $\text{d}^8 \text{ Co, Rh, and Ru}$  half-sandwich complexes  $\text{MCpL}_2$  or  $\text{M}(\text{arene})\text{L}_2$ ,<sup>13</sup> whereas protonation and electrophilic addition to nickelocene<sup>14</sup> or its methyl derivatives<sup>15</sup> exclusively occurs at the Cp ring, leading to the exo-substituted cyclopentadienyl complexes<sup>15</sup> or to follow-up products thereof.<sup>14</sup>

A mechanism initiated by Cp protonation leading to **1<sup>+</sup>** and  $\text{H}_2$  is depicted as mechanism I in Scheme I, eq 8–10. The hydrogen-producing step in this mechanism is the proton-hydride reaction (eq 10) of the neutral complex **4**, generated through reduction of **4<sup>+</sup>** by **1**. Note that **4** (along with **1<sup>+</sup>**) would also be the product of the familiar two-step oxidative addition of an electrophile "HX" to cobaltocene ("RX reaction"). Though **4**

(9) Koelle, U.; Khouzami, F.; Fuss, B. *Angew. Chem., Int. Ed. Engl.* **1982**, *21*, 131; *Angew. Chem. Suppl.* **1982**, 230–240.

(10) Koelle, U.; Khouzami, F. *Angew. Chem., Int. Ed. Engl.* **1980**, *19*, 640.

(11) It was checked by control experiments at high pH that clustering of the neutral sandwiches was not responsible for the remaining absorption.

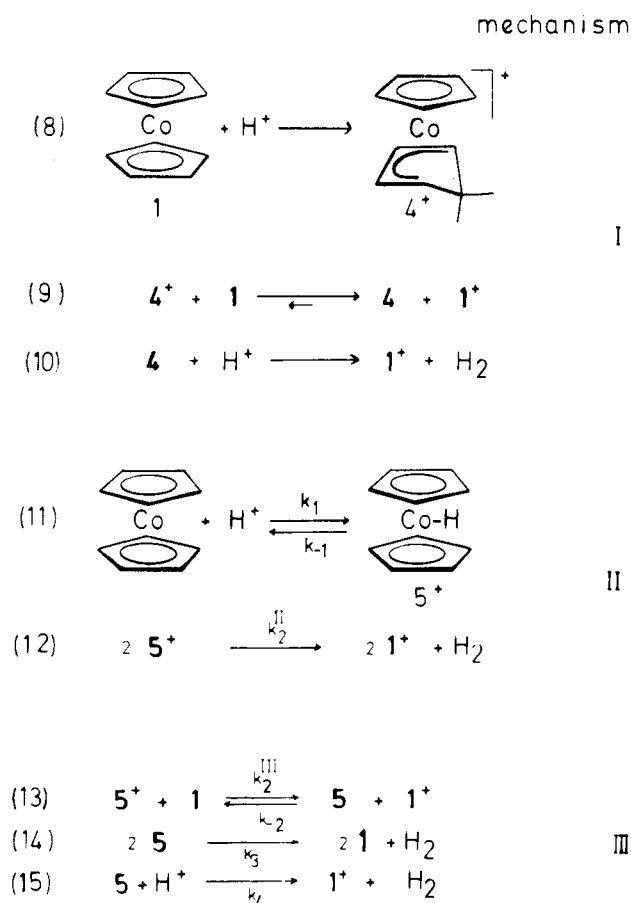
(12) Deeming, A. J. In ref 1, Vol. 4, p 483 ff.

(13) Werner, H. *Angew. Chem., Int. Ed. Engl.* **1983**, *22*, 927 and references given therein.

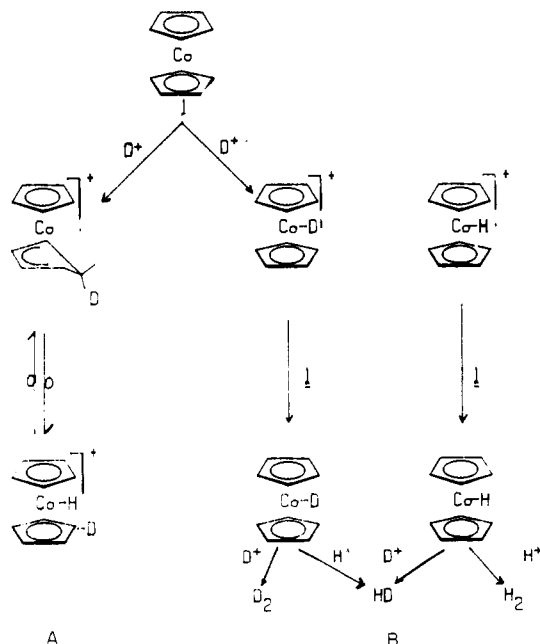
(14) Court, T. L.; Werner, H. *J. Organomet. Chem.* **1975**, *102*, C9.

(15) Koelle, U.; Khouzami, F. *Chem. Ber.* **1982**, *115*, 1178.

## Scheme I



## Scheme II



has been reported to be acid-sensitive<sup>16</sup> we found that its reaction with acid (see Experimental Section) is slow and incomplete under conditions where 1-3 readily react, discarding mechanism I. Initial Cp protonation with subsequent hydrogen transfer to the metal as given in Scheme II (route A) is disproved by the deuteration experiment. In the case of metal protonation (route B) the isotopic composition determined by statistics, assuming excess hydrogen

Table II. Limiting Rate Constant Ratios for Mechanisms II and III<sup>a</sup>

limiting condition	II	III
$k_1/k_{-1}$	$\geq 10 \text{ M}^{-1}$	$\geq 20 \text{ M}^{-1}$
$k_1/k_2$	$\leq 5 \times 10^{-7}$	$\leq 2 \times 10^{-6}$
$k_1^{\text{expl } b}$	$40 \text{ s}^{-1} \text{ M}^{-1}$	$22 \text{ s}^{-1} \text{ M}^{-1}$

<sup>a</sup>  $k_2 = 10^8 \text{ s}^{-1} \text{ M}^{-1}$ . <sup>b</sup> Rate constant for protonation which reproduces  $k_{\text{obsd}}$ .

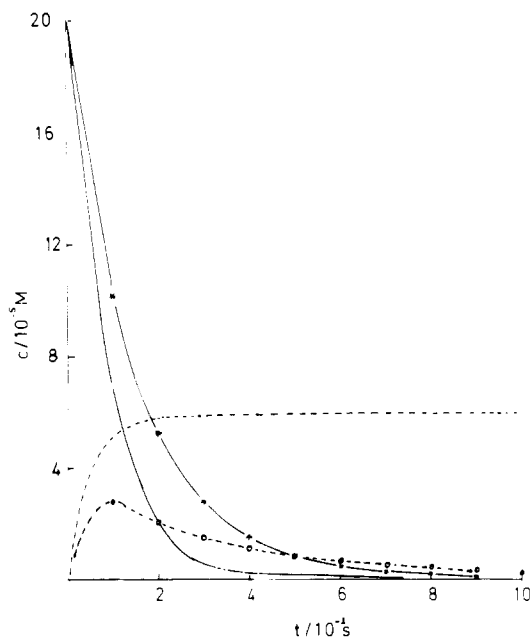


Figure 6. Decay of [C] and [CH<sup>+</sup>] simulated numerically with parameters  $[C]_0 = 2 \times 10^{-5} \text{ M}$ ,  $[H^+] = 0.48 \text{ M}$ ,  $[C^+]_0 = 3.5 \times 10^{-3} \text{ M}$ ,  $k_1 = 1.5 \times 10^2 \text{ M}^{-1} \text{ s}^{-1}$ ,  $k_{-1} = 15 \text{ s}^{-1}$ , and  $k_2 = 10^7 \text{ M}^{-1} \text{ s}^{-1}$ . Mechanism II: (-\*-) C; (---) CH<sup>+</sup>. Mechanism III: (—) C; (···) CH<sup>+</sup>.

coming from the reagents, requires an H<sub>2</sub>:HD:D<sub>2</sub> ratio of 0.45:2.85:10.42, i.e. slightly less H<sub>2</sub> than observed (see Experimental Section). This points to a small isotope effect that favors H<sub>2</sub> over HD and D<sub>2</sub>. In addition the absence of any deuterium in the cobaltocenium salt is conclusive proof for metal protonation.

From the metal-protonated species 5<sup>+</sup> hydrogen could then be generated by a second-order disproportionation, mechanism II (eq 12), or by reduction of 5<sup>+</sup> by 1 to generate the 19-electron intermediate 6 (eq 13), which could rapidly release hydrogen by either 14 or 15, designated as mechanism III in Scheme I. The last two pathways have been established for the reaction of the 19-electron hydridic intermediates CoCp(PR<sub>3</sub>)<sub>2</sub>H.<sup>17</sup> Depicted in Scheme II is the generation of hydrogen based on mechanism III, which accounts for the formation of D<sub>2</sub>, HD, and H<sub>2</sub> observed in the deuteration experiment. The same isotopic distribution would of course emerge from mechanism II.

Rate equations for mechanisms II (eq 16 and 17) and III (eq 18 and 19), where (13) was treated as a forward reaction only, have been simulated numerically for a particular case (last entry of the first part in Table I) in order to obtain limiting values for the individual rate constants which reproduce the experimental findings, where C and CH<sup>+</sup> represent cobaltocenium and protonated cobaltocenium

$$d[C]/dt = -k_1[C][H^+] + k_{-1}[CH^+] \quad (16)$$

$$d[CH^+]/dt = k_1[C][H^+] - k_{-1}[CH^+] - k_2^{III}[CH^+]^2 \quad (17)$$

mechanism III

$$d[C]/dt = k_{-1}[CH^+] - k_1[C][H^+] - k_2^{III}[C][CH^+] \quad (18)$$

$$d[CH^+]/dt = -k_1[C][H^+] - k_{-1}[CH^+] + k_2^{III}[C][CH^+] \quad (19)^{18}$$

(16) See ref 2, p 481.

(17) Koelle, U.; Ohst, S. *Inorg. Chem.* **1986**, *25*, 2689.

cobaltocene, respectively. Besides reproduction of the experimental rate constant  $k_{\text{obsd}}$  the simulation has to conform to a first-order reaction and an absorption decay to the initial value, which implies that  $5^+$  is not accumulated during the reaction, i.e.  $[\text{CH}^+] \lesssim 0.1[\text{C}]$  throughout. Results of the numerical simulations are compiled in Table II. For mechanism II  $k_1/k_2^{\text{II}} \leq 5 \times 10^{-7}$  is required to keep  $[\text{CH}^+] \ll [\text{C}]$ . A first-order decay then obtains for  $k_1/k_{-1} > 10 \text{ M}^{-1}$ . Mechanism III similarly requires  $k_1/k_2^{\text{III}} \leq 2 \times 10^{-6}$  to keep  $[\text{CH}^+]$  sufficiently low and  $k_1/k_{-1} > 20 \text{ M}^{-1}$  to ensure first-order behavior.

A difference between both mechanisms becomes evident if the ratio  $k_1/k_2$  is increased by increasing  $k_1$ . In mechanism II this causes a deviation of  $d[\text{C}]/dt$  toward higher order, where both  $[\text{C}]$  and  $[\text{CH}^+]$  smoothly decay (Figure 6). In contrast, for mechanism III there is a steep decay of  $[\text{C}]$ , whereas  $[\text{CH}^+]$  after a short time reaches a nearly constant level (Figure 6). As can be seen intuitively from the reaction equations, in mechanism II  $[\text{C}]$  and  $[\text{CH}^+]$  will decay smoothly at all realistic  $k$  values, whereas in mechanism III the disappearance of  $[\text{CH}^+]$  becomes very slow once  $[\text{C}]$  is exhausted. The point in the reaction course at which this occurs and thus the remaining concentration of  $[\text{CH}^+]$  is critically dependent on  $k_1/k_2$  and also on the initial concentration of neutral cobaltocene.<sup>19,20</sup> The latter case obviously

conforms to the behavior found for **2** and **3**. If the increase in  $k_1$  by a factor of 300 when one proceeds from **1** to **2**, as borne out by the experiment in ethanol at low proton concentration, leads to an increase in  $k_1/k_2$ , buildup of  $[\text{CH}^+]$  would be a consequence and the absorption decay of Figure 5 results with  $[\text{CH}^+]$  as the slowly decaying species. The kinetic behavior of **2** and **3** is thus better accounted for by mechanism III. In chemical terms this implies a higher rate of protonation for the methylated cobaltocenes. The electron-releasing effect of the methyl groups is expected to increase the metal Brønsted basicity, and it appears to be this effect rather than the more negative redox potentials<sup>10</sup> that is responsible for the faster reaction of these latter sandwich complexes.

Note that  $k_2^{\text{II}}$  ( $>10^7$ – $10^8 \text{ s}^{-1} \text{ M}^{-1}$ ) represents the rate constant for a bimolecular reaction of two cations, whereas  $k_2^{\text{III}}$  is the rate constant for electron transfer between a neutral and a cationic sandwich molecule, which, by virtue of its low reorganization energy, is believed to be very rapid.

In either mechanism it is essential to note that the observed first-order behavior implies the protonation step in the overall reaction to be rate-determining with  $k_{\text{obsd}}$  largely representing the rate of metal protonation (Table II). Obviously the value found for  $k_1$  is considerably reduced from rates common for p-lone-pair bases, which generally protonate near the diffusion limit. Precedence for slow protonation at transition-metal centers has again been found with the complex  $\text{CoCp}(\text{PPh}_3)_2$ ,<sup>17</sup> and a few more values that testify to the generality of a reduced protonation rate at coordinatively saturated transition-metal centers can be found in the literature.<sup>22</sup> Considering the role of transition-metal complexes as catalysts for proton reduction<sup>23</sup> as well as other catalytic reactions featuring electrophilic attack at a basic metal center as the rate-determining step, this observation appears of paramount importance since it may well determine the overall catalytic activity of a complex.

**Registry No.** **1**, 1277-43-6; **2**, 97210-32-7; **3**, 74507-62-3;  $\text{D}_2$ , 7782-39-0;  $\text{H}^+$ , 12408-02-5.

- (18) Since buildup of CH is not realistic,  $k_3, k_4 \gg k_{-2}$  was assumed and back electron transfer neglected.
- (19) The same argument may be derived from an analysis of eq 19 and 20. These equations yield a relation between  $[\text{C}]_0$ ,  $[\text{C}]$ , and  $[\text{CH}^+]$  (see: Benson, S. W. *The Foundations of Chemical Kinetics*; McGraw-Hill: New York, 1960; p 43 ff), i.e.  $[\text{CH}^+]/K + 2 \ln(1 - [\text{CH}^+]/K) = -[\text{C}]_0/K(1 - [\text{C}]/[\text{C}]_0)$ , where  $K = k_1[\text{H}^+]/k_2^{\text{III}}$ , which for  $t \rightarrow \infty$  leads to  $[\text{CH}^+]_{\infty}/K + 2 \ln(1 - [\text{CH}^+]_{\infty}/K) = -[\text{C}]_0/K$ . When  $[\text{CH}^+]_{\infty}$  vs  $K$  is plotted, it is seen that, depending on  $[\text{C}]_0$ ,  $[\text{CH}^+]_{\infty}$  reaches a constant level once  $K$  has increased over a critical value.
- (20) An assumption implemented in mechanism III, the condition  $k_3, k_4 \geq k_{-2}^{\text{III}}$ , requires that the redox equilibrium (13) lie not too far to the left. Although there appears no way to determine experimentally the redox potential of the couple  $\text{CH}^{+/0}$ , we learned from our study of protonated cobalt complexes  $\text{CpCo}(\text{PR}_3)_2\text{H}^+$ <sup>17</sup> that the  $\text{CH}^{+/0}$  redox potentials are generally negative from the  $\text{C}^{+/0}$  potentials, but in cases where the difference  $E_{1/2}(\text{C}^{+/0}) - E_{1/2}(\text{CH}^{+/0})$  is more than about 300 mV stable protonated complexes  $\text{CH}^+$  ensue rather than oxidation of C to  $\text{C}^+$  by protons,<sup>21</sup> even though the  $\text{C}^{+/0}$  redox potential would be thermodynamically highly sufficient for proton reduction. The potential difference  $E_{1/2}(\text{C}^{+/0}) - E_{1/2}(\text{CH}^{+/0}) < 300 \text{ mV}$  for the cobaltocenes would still be compatible with the above requirement.
- (21) A recent example was found with the compound  $\text{CoCp}(\text{bpy})$ , which is oxidized by protons to  $\text{CoCp}(\text{bpy})^+$  (Koelle, U.; Ohst, S., to be submitted for publication), where, by electrochemistry, the  $\text{CH}^{+/0}$  redox potential was located about 200 mV negative from the  $\text{C}^{0/+}$  potential.

- (22)  $k_1$  ( $\text{M}^{-1} \text{ s}^{-1}$ ) for protonation: (a)  $\text{CoCp}(\text{PPh}_3)_2$  (electroanalytically), 30–40;<sup>17</sup> (b)  $(\text{CoCp}(\mu\text{-PPh}_2))_2$  (stopped flow), 270 (Koelle, U., unpublished results); (c)  $\text{Rh}(\text{dmgH})_2\text{PPh}_3^-$  (stopped flow), 36 (Ramasami, T.; Espenson, J. H. *Inorg. Chem.* **1980**, *19*, 1864); (d)  $\text{IrCl}_2\text{CO}(\text{PPh}_3)_2^-$  (stopped flow), 553 (Pearson, R. G.; Kresge, C. T. *Inorg. Chem.* **1981**, *20*, 1878).
- (23) (a) See: Krishnan, C. V.; Brunshwig, B. S.; Creutz, C.; Sutin, N. *J. Am. Chem. Soc.* **1985**, *107*, 2005 and literature cited therein. (b) Koelle, U.; Grätzel, M. *Angew. Chem., Int. Ed. Engl.* **1987**, *26*, 567.